LETTER

doi:10.1038/nature10539

A SUMOylation-defective MITF germline mutation predisposes to melanoma and renal carcinoma

Corine Bertolotto[1,2,3]*, Fabienne Lesueur[4]†*, Sandy Giuliano[1,2]*, Thomas Strub[5], Mahaut de Lichy[4], Karine Bille[1], Philippe Dessen[6], Benoit d'Hayer[4], Hamida Mohamdi[7,8,9], Audrey Remenieras[4]†, Eve Maubec[7,10], Arnaud de la Fouchardière[11], Vincent Molinié[12], Pierre Vabres[13], Stéphane Dalle[14], Nicolas Poulalhon[14], Tanguy Martin-Denavit[14], Luc Thomas[14], Pascale Andry-Benzaquen[15], Nicolas Dupin[15], Françoise Boitier[15], Annick Rossi[16], Jean-Luc Perrot[17], Bruno Labeille[17], Caroline Robert[18], Bernard Escudier[18], Olivier Caron[18], Laurence Brugières[19], Simon Saule[20], Betty Gardie[21], Sophie Gad[21], Stéphane Richard[21,22], Jérôme Couturier[23], Bin Tean Teh[24,25], Paola Ghiorzo[26], Lorenza Pastorino[26], Susana Puig[27], Celia Badenas[27], Hakan Olsson[28], Christian Ingvar[29], Etienne Rouleau[30], Rosette Lidereau[30], Philippe Bahadoran[3], Philippe Vielh[31], Eve Corda[7,9], Hélène Blanché[9], Diana Zelenika[32], Pilar Galan[33], The French Familial Melanoma Study Group‡, Valérie Chaudru[7,9,34], Gilbert M. Lenoir[4,35], Mark Lathrop[9,32], Irwin Davidson[5], Marie-Françoise Avril[15], Florence Demenais[7,8,9], Robert Ballotti[1,2,3]* & Brigitte Bressac-de Paillerets[4,7]*

So far, no common environmental and/or phenotypic factor has been associated with melanoma and renal cell carcinoma (RCC). The known risk factors for melanoma include sun exposure, pigmentation and nevus phenotypes[1]; risk factors associated with RCC include smoking, obesity and hypertension[2]. A recent study of coexisting melanoma and RCC in the same patients supports a genetic predisposition underlying the association between these two cancers[3]. The microphthalmia-associated transcription factor (*MITF*) has been proposed to act as a melanoma oncogene[4]; it also stimulates the transcription of hypoxia inducible factor[5] (*HIF1A*), the pathway of which is targeted by kidney cancer susceptibility genes[6]. We therefore proposed that *MITF* might have a role in conferring a genetic predisposition to co-occurring melanoma and RCC. Here we identify a germline missense substitution in *MITF* (Mi-E318K) that occurred at a significantly higher frequency in genetically enriched patients affected with melanoma, RCC or both cancers, when compared with controls. Overall, Mi-E318K carriers had a higher than fivefold increased risk of developing melanoma, RCC or both cancers. Codon 318 is located in a small-ubiquitin-like modifier (SUMO) consensus site (ΨKXE) and Mi-E318K severely impaired SUMOylation of MITF. Mi-E318K enhanced MITF protein binding to the *HIF1A* promoter and increased its transcriptional activity compared to wild-type MITF. Further, we observed a global increase in Mi-E318K-occupied loci. In an RCC cell line, gene expression profiling identified a Mi-E318K signature related to cell growth, proliferation and inflammation. Lastly, the mutant protein enhanced melanocytic and renal cell clonogenicity, migration and invasion, consistent with a gain-of-function role in tumorigenesis. Our data provide insights into the link between SUMOylation, transcription and cancer.

MITF encodes a member of the Myc supergene family of basic helix–loop–helix zipper transcription factors. It has a complex intron–exon structure, yielding protein products with different amino termini[7]. The M-isoform (expressed in the melanocyte lineage) of MITF regulates expression of a large set of genes promoting proliferation and invasion. For instance, it controls the expression of *MET*[5] and *CDKN2A/p16INK4A*[5], which have key roles in melanoma development. The role of the A-isoform of MITF (expressed in kidney) in renal cell transformation has yet to be elucidated. However, *MITF* belongs to the same family of transcription factors (the MiT family) as the *TFEC*, *TFE3* and *TFEB* genes; the two latter were identified as targets of somatic recurrent translocations in a RCC subtype found predominantly in children and young adults[8].

We sequenced the *MITF* gene in 62 patients with melanoma and RCC. Five patients exhibited a germline heterozygous missense substitution, p.E318K (c.952G>A, in MITF isoform 4, NCBI accession NM_000248.3) (Fig. 1a). The frequency of this variant was significantly higher in patients with both melanoma and RCC (melanoma + RCC) than in 1,659 population-based cancer-free controls ($P = 1.3 \times 10^{-4}$). Carriers of the p.E318K variant (Mi-E318K) exhibited a 14-fold higher risk than controls for developing melanoma + RCC (Table 1). To investigate the effect of Mi-E318K on susceptibility to melanoma alone, we genotyped 603 affected patients that had undergone oncogenetic testing for melanoma susceptibility genes[1] and were negative for *CDKN2A* and *CDK4* mutations (Table 1). Mi-E318K

[1]INSERM, U895 (équipe 1), Equipe labélisée Ligue Contre le Cancer, C3M, 06204 Nice, France. [2]Université of Nice Sophia-Antipolis, UFR Médecine, 06204 Nice, France. [3]Centre Hospitalier Universitaire de Nice, Service de Dermatologie, 06204 Nice, France. [4]Service de Génétique, Institut de Cancérologie Gustave Roussy, 94805 Villejuif, France. [5]Institut de Génétique et de Biologie Moléculaire et Cellulaire, CNRS, INSERM, Université de Strasbourg, 67404 Illkirch, France. [6]INSERM, UMR985, Institut de Cancérologie Gustave Roussy, 94805 Villejuif, France and Université Paris-Sud 11, 91405 Orsay. [7]INSERM, U946, Genetic Variation and Human Diseases Unit, 75010 Paris, France. [8]Université Paris Diderot, Sorbonne Paris Cité, Institut Universitaire d'Hématologie, 75010 Paris, France. [9]Fondation Jean Dausset-Centre d'Etude du Polymorphisme Humain (CEPH), 75010 Paris, France. [10]AP-HP, Hôpital Bichat, Service de Dermatologie, Faculté Paris Diderot, 75018 Paris, France. [11]Département de Pathologie, Centre Léon Bérard, 69008 Lyon, France. [12]Department of Pathology, Hôpital Saint-Joseph, 75014 Paris, France. [13]Department of Dermatology, Centre Hospitalier Universitaire, 21079 Dijon, France. [14]Lyon 1 University and Centre Hospitalier Lyon Sud, Department of Dermatology, 69495 Pierre Bénite, France. [15]AP-HP, Hôpital Cochin -Tarnier, Service de Dermatologie and Université Paris Descartes, 75006 Paris, France. [16]Unité de Génétique Clinique, Hôpital Charles Nicolle, CHU Rouen, 76038 Rouen, France. [17]Department of Dermatology, CHU Hôpital Nord, 42055 Saint-Etienne, France. [18]Department of Medicine, Institut de Cancérologie Gustave Roussy, 94805 Villejuif, France. [19]Department of Pediatry, Institut de Cancérologie Gustave Roussy, 94805 Villejuif, France. [20]Institut Curie, CNRS UMR33 and INSERM U1021, Université Paris-Sud 11, 91405 Orsay, France. [21]Génétique Oncologique EPHE-INSERM U753, Faculté de Médecine, Université Paris-Sud 11 and Institut de Cancérologie Gustave Roussy, 94805 Villejuif, France. [22]Centre Expert National Cancers Rares PREDIR, INCa/AP-HP, Service d'Urologie, Hôpital de Bicêtre, 94275 Le Kremlin-Bicêtre, France. [23]Service de Génétique, Institut Curie, 75005 Paris, France. [24]Laboratory of Cancer Genetics, Van Andel Research Institute, Grand Rapids, 49503 Michigan, USA. [25]NCCS-VARI Translational Research Laboratory, National Cancer Center Singapore, 16910 Singapore. [26]Department of Internal Medicine, University of Genoa, 16132 Genoa, Italy. [27]Dermatology Department and Biochemistry and Molecular Genetics, Melanoma Unit, Hospital Clinic, IDIBAPS, and CIBER de Enfermedades Raras, Instituto de Salud Carlos III, 08036 Barcelona, Spain. [28]Department of Oncology, Lund University and Hospital, Lund, 22185 Sweden. [29]Department of Surgery, Lund University and Hospital, Lund, 22185 Sweden. [30]Service d'Oncogénétique, Hôpital René Huguenin- Institut Curie, 92210 Saint-Cloud, France. [31]Department of Pathology, Translational Research Laboratory and Biobank, Institut de Cancérologie Gustave Roussy, 94805 Villejuif, France. [32]Commissariat à l'Energie Atomique, Centre National de Génotypage, 91057 Evry, France. [33]INSERM, UMR557, INRA U1125, CNAM, Paris 13, CRNH Idf, 93000 Bobigny, France. [34]Université d'Evry Val d'Essonne, 91025 Evry, France. [35]Université Paris-Sud 11, Faculté de Médecine, 94275 Le Kremlin-Bicêtre, France. †Present addresses: Genetic Cancer Susceptibility group, International Agency for Research on Cancer, 69372 Lyon, France (F.L.); Genetic Department, Institut Paoli Calmettes, 13273 Marseille, France (A.R.).

*These authors contributed equally to this work.

‡A list of authors and their affiliations appears at the end of the paper.

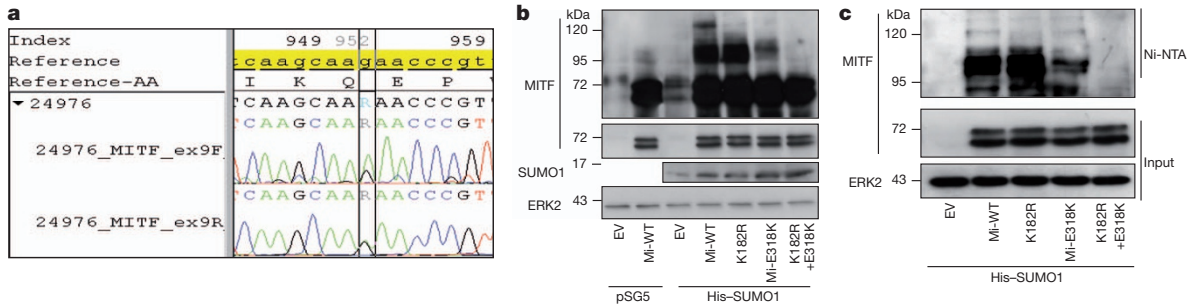

Figure 1 | Mi-E318K mutation impairs MITF SUMOylation. a, *MITF* sequence data of the c.952G>A, p.E318K germline substitution (Mi-E318K). **b**, HEK293 cells were co-transfected with empty pcDNA3 vector (EV) or pcDNA3 encoding wild-type (Mi-WT) or mutant (K182R, Mi-E318K or K182R+E318K) Myc-tagged MITF and either with an empty vector or His–SUMO1 pSG5 vectors. Western blot analysis with antibodies to MITF, SUMO1 and ERK2 used as a loading control. **c**, Western blot analysis with antibodies to MITF and ERK2 of protein extracts before (Input) and after Ni-NTA affinity purification.

frequency was significantly higher in these patients than in controls ($P = 7.8 \times 10^{-5}$). The carriers of Mi-E318K in this group exhibited >4-fold higher melanoma risk than controls (Table 1). In addition, Mi-E318K co-segregated with melanoma in three melanoma-prone families that had DNA available in relatives of index cases carrying Mi-E318K (Supplementary Fig. 1a). We also found that Mi-E318K was more strongly associated with multiple occurrences of primary melanomas than with single occurrence, irrespective of family history ($P = 0.02$, Supplementary Table 1). To investigate the effect of Mi-E318K in RCC susceptibility, we genotyped 164 patients with RCC referred to oncogenetic clinics, who were enriched for rare histological subtypes and who were wild type for the known RCC-predisposing genes[6]. These patients also exhibited a higher frequency of Mi-E318K than controls ($P = 0.008$) (Table 1). After correcting for multiple testing, the association between Mi-E318K and melanoma + RCC, melanoma only or RCC only remained significant, although marginally so for the RCC-only group ($P = 0.02$). The three groups showed similar Mi-E318K allele frequencies ($P = 0.10$). When all 829 patients with melanoma and/or RCC were pooled, Mi-E318K frequency was significantly different from controls ($P = 1.2 \times 10^{-6}$). The pooled group of Mi-E318K carriers had a greater than fivefold risk of developing melanoma, RCC or both cancers, as compared to controls (Table 1). The clinical and pathological features of the 27 Mi-E318K carriers are described in Supplementary Table 2. Principal component analysis (PCA) of single nucleotide polymorphism (SNP) data across the genome in more than 75% of cases and controls showed appropriate clustering of cases and controls after exclusion of a few subjects of non-European ancestry (Supplementary Fig. 1b). Association analysis of melanoma and/or RCC with Mi-E318K provided similar results when performed with or without adjusting for principal components (Supplementary Table 3). To assess whether Mi-E318K predisposed to the coexistence of melanoma and a second primary neoplasm other than RCC, we gathered data from European countries, but these data were insufficient for separate analyses of each type of cancer. Overall, we concluded from our findings that Mi-E318K is a rare substitution that confers an increased risk for developing melanoma and/or RCC. However, given the selection of patients who were part of case series undergoing genetic testing, further investigation of Mi-E318K in large series of unselected sporadic renal cancer and melanoma cases is merited.

Previous studies have shown that MITF is expressed in a majority of melanomas and in a subset of kidney tumours[9]. Accordingly, our immunohistochemical analyses showed that MITF was expressed in both melanomas from patients carrying the germline mutation Mi-E318K ($n = 8$) and in melanomas from wild-type patients ($n = 8$) (Supplementary Fig. 2a, b). In addition, two out of seven RCCs from Mi-E318K carriers were positive for MITF (Supplementary Fig. 2c, d), suggesting that Mi-E318K might have a role in renal transformation. None of the six wild-type MITF RCC samples analysed in this study showed MITF labelling.

Mi-E318K occurs at a conserved position in MITF within a consensus motif (IKQE) that matches perfectly with the consensus sequence ΨKXE for covalent binding of SUMO[10] (Supplementary Fig. 3a, b). Because SUMOylation is critically dependent on the acidic residue at +2 (E) of the acceptor lysine (K), we tested whether Mi-E318K affects MITF SUMOylation. Co-expression of histidine-tagged (His)–SUMO1 with wild-type MITF and western blot analysis revealed a 120-kDa band and a doublet above 95 kDa, in addition to the 55–65 kDa native doublet (Fig. 1b). The p.K182R mutation introduced within the second MITF SUMOylation site led to complete disappearance of the 120-kDa MITF form, but had little effect on the 95-kDa doublet. When glutamic acid residue 318 was replaced by a lysine, mimicking the germline mutation, we observed a strong decrease in the levels of all the SUMO-modified forms of MITF. Lastly, no SUMOylated forms were seen with the double-mutant [p.K182R;p.E318K]. Similar observations were made with co-expression of haemagglutinin-tagged (HA)–SUMO2 (Supplementary Fig. 4a), demonstrating that Mi-E318K affected both SUMO1 and SUMO2 modifications. Western blot analysis with anti-MITF antibody, after affinity purification of His–SUMO1-containing proteins on Ni-NTA columns, confirmed that the high molecular weight bands were indeed SUMO-modified MITF proteins and that Mi-E318K markedly reduced all the MITF SUMOylated forms (Fig. 1c). Altogether, these results demonstrated that codon 316 was the major SUMO acceptor site in MITF and that Mi-E318K severely impaired SUMO conjugation to MITF.

SUMOylation has been shown to orchestrate a variety of cellular processes, in part through the control of nucleo-cytoplasmic signal transduction. However, both Mi-E318K and wild type were detected

Table 1 | Frequency of the germline Mi-E318K substitution

Subjects	Number of non-carriers	Number of carriers‡	Total	Frequency of p.E318K	FET *P* value†	OR (95%CI)*
Controls	1,649	10	1,659	0.003	-	Reference
Patients with melanoma and/or RCC	802	27	829§	0.016	1.2×10^{-6}	5.55 (2.59–12.91)
Melanoma + RCC	57	5	62	0.040‖	1.3×10^{-4}	14.46 (3.74–48.04)
Melanoma only	586	17	603	0.014‖	7.8×10^{-5}	4.78 (2.05–11.75)
RCC only	159	5	164	0.015‖	0.008	5.19 (1.37–16.87)

* OR (95% CI) is the odds ratio (with 95% confidence interval) associated with the Mi-E318K carrier status.
† FET, Fisher's exact test for the difference in Mi-E318K allele frequency between each group of patients and controls.
‡ All carriers are heterozygotes for the Mi-E318K substitution. Clinical and pathological features of the 27 carriers are described in Supplementary Table 2.
§ A full description of the 829 patients is given in Methods.
‖ The Fisher's exact test showed no significant differences ($P = 0.10$) in allele frequency among the three groups of patients (melanoma + RCC, melanoma only, RCC only).

by immunofluorescence in the nucleus of transfected melanoma cells. This indicated that Mi-E318K did not affect MITF nuclear localization (Supplementary Fig. 4b, c).

Previous reports indicated that SUMOylation of MITF repressed its transcriptional activity, particularly when the targeted promoter contained multiple E-boxes[10]. Indeed, on a synthetic reporter gene comprising three E-boxes, Mi-E318K showed two- to threefold greater transcriptional activity than that of wild type (Fig. 2a). The double MITF mutant, [p.E318K;p.K182R], was more effective than Mi-E318K, and the single p.K182R mutant exhibited activity comparable to that of wild type. We next tested whether Mi-E318K affected MITF activity on physiological target promoters, such as *MET* and *HIF1A*, two MITF-regulated genes involved in cell survival and in melanocyte and kidney tumorigenesis. We also tested *CDKN2A* and *TYR* promoters, which are involved in melanocyte proliferation and differentiation processes, respectively. Wild type and mutant Mi-E318K showed similar activity on the *MET* (Fig. 2b), *TYR* and *CDKN2A* promoters (Supplementary Fig. 5), but Mi-E318K more efficiently activated the *HIF1A* promoter than wild type (Fig. 2c). This observation suggests that Mi-E318K alters MITF transcriptional activity on a subset of its target genes. To determine the global transcriptional effects of Mi-E318K, we performed pan-genomic expression profiling of A375 melanoma and RCC4 cells infected with adenoviruses that encoded either wild-type MITF or Mi-E318K (Supplementary Fig. 6a, b, c, d). Analysis of the genes regulated differentially by wild type and Mi-E318K in

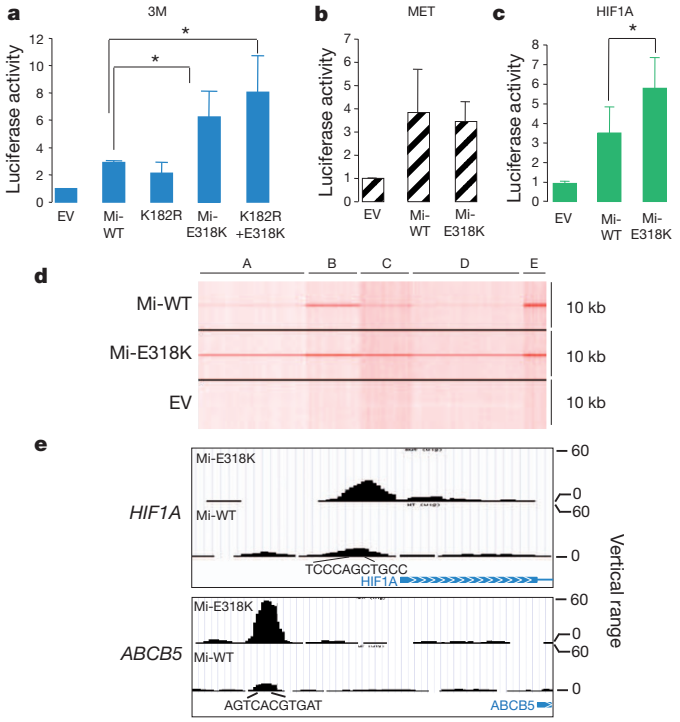

Figure 2 | Mi-E318K increases MITF binding and transcriptional regulation of a subset of its target genes. **a**–**c**, Reporter plasmids containing the luciferase gene under the control of different MITF target promoters were co-expressed with empty pcDNA3 (EV) or pcDNA3 encoding wild-type (Mi-WT) or mutant (K182R, Mi-E318K, K182R+E318K) MITF. **a**, HEK293 cells were transfected with a 3M-box reporter. **b**, **c**, 501mel human melanoma cells were transfected with the *c-MET* promoter reporter (**b**) or the *HIF1A* promoter reporter (**c**). The results were expressed as the fold stimulation over basal luciferase activity. Data represent the mean + s.d. of three independent experiments. Asterisk indicates a statistically significant difference (Student's *t*-test, $P \leq 0.05$). **d**, MITF-occupied loci in genomic DNA extracted from 501mel melanoma cells expressing Mi-WT or Mi-E318K. MITF tag density was compared in the region of ±5 kb around the MITF-occupied loci. **e**, University of California Santa Cruz (UCSC) view of MITF occupancy of *HIF1A* and *ABCB5* loci. The blue bar with arrowheads below each panel indicates the transcription start site; the E-box nucleotide sequence is shown under peaks.

A375 cells failed to identify a specific Mi-E318K signature. However, in RCC4 cells, we identified a Mi-E318K signature composed of 32 genes (Supplementary Table 4). On the basis of the bioinformatic analysis using Ingenuity Pathways Analysis (IPA) software, these genes were associated with cell growth, proliferation and inflammation (Supplementary Fig. 7). Among the genes downregulated by Mi-E318K compared to wild type, *IRAK2* (ref. 11), *EGR1* (ref. 12) and *IL6* (ref. 13) have tumour suppressor functions. The upregulated genes included *CCR7*, a HIF-1α target gene[14] and activator of the NFκB pathway[15]; *ABCB5*, one of the most well-documented markers for melanoma initiating cells[16]; *GADD45G*, a member of the GADD45 family of stress sensors, which connects NFκB to the MAP kinase pathway[17]; and *TRIM63*, which was one of the top five upregulated genes and was the major gene found to be differentially expressed in patients with TFE3/TFEB translocation RCC as compared to other subtypes of RCC[8]. These experiments confirmed the different transcriptional potentials of wild type and Mi-E318K, particularly on genes involved in proliferation and inflammation.

To investigate whether SUMOylation influenced genome-wide MITF occupancy of its target sites, we performed chromatin immunoprecipitation coupled to high-throughput sequencing (ChIP-seq) experiments in 501mel human melanoma cell lines expressing wild type or Mi-E318K. Data analysis shows that 22,157 sites are occupied by Mi-E318K, whereas only 9,107 were detected for wild type, the difference being the presence of a large number of weakly occupied sites in the Mi-E318K data set. Comparative analysis of the ChIP-seq data sets using read density matrix clustering identified sites that are occupied by both wild type and Mi-E318K (Fig. 2d, sets B and E), whereas some promoter sites are uniquely or preferentially occupied by Mi-E318K (Fig. 2d, sets A and D; Supplementary Table 5). For example, a higher occupancy of the *HIF1A* promoter by Mi-E318K compared to wild type is observed (Fig. 2e). Mi-E318K also showed increased binding to the *ABCB5* locus (Fig. 2e), the expression of which is increased in RCC4-expressing Mi-E318K. Of note, Mi-E318K binds more efficiently than wild type to the *HMOX1* promoter (Supplementary Table 5), a gene involved in both kidney cancer[18] and melanoma cell growth[19]. Although the *HIF1A* promoter was better occupied and activated (in a gene promoter assay) by Mi-E318K than by wild type, we observed equal amounts of *HIF1A* messenger RNA in Mi-E318K- or wild-type-infected A375 and RCC4 cells. HIF1A transcripts are subjected to post-transcriptional regulation that controls their stability[20]; this may mask the transcriptional effect of Mi-E318K. Alternatively, the cellular context or the chromatin landscape in RCC4 or A375 cells may not permit increased transcription. Indeed, this was observed for MITF target genes such as *TYR*, *TYRP1* and *DCT*, which were not upregulated by MITF overexpression in A375 cells. Taken together, our data indicate that the naturally occurring Mi-E318K severely impaired MITF SUMOylation and showed higher global transcriptional activity, in agreement with the currently accepted model of SUMO-mediated transcriptional repression[21]. The global increase in Mi-E318K-occupied loci coupled with the existence of sites exclusively bound by the mutant protein indicate that SUMOylation regulates the repertoire of MITF target genes. SUMOylation-deficient Mi-E318K protein may therefore result in the regulation of distinct sets of genes, hence leading to gain-of-function properties.

To evaluate the tumorigenic potential of Mi-E318K, we tested its effect on migration, invasion and colony formation of stable melanoma cells (501mel) expressing wild-type MITF or Mi-E318K (Fig. 3a). We observed increased migration (Fig. 3b) and invasion (Fig. 3c) in two different Mi-E318K clones compared to wild-type clones. Similar results were obtained in VHL-deficient RCC4 cells (Fig. 3d, e) infected with adenoviruses encoding wild type or Mi-E318K. In contrast, Mi-E318K caused barely significant effects in A375 cells (used also for expression profiling) (Supplementary Fig. 8). Lastly, in a colony-forming assay with immortalized murine melanocytes, Melan-a (Fig. 3f), and RCC4 cells (Fig. 3g), the number of colonies after transfection of

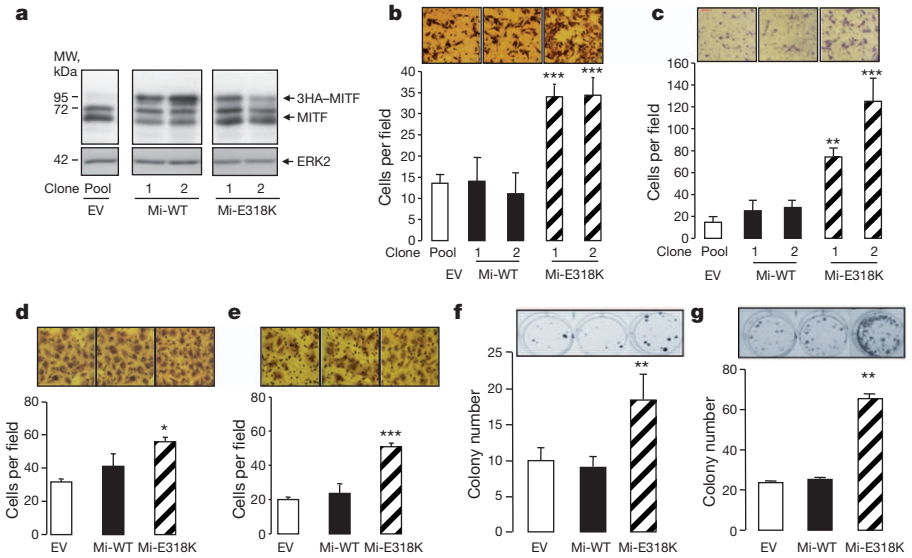

Figure 3 | Mi-E318K-enhanced migration, invasion and clonogenicity of melanoma and renal cancer cells. **a**, Western blot analysis with antibodies to MITF or ERK2 of 501mel cells stably transfected with empty vector (EV), or vector encoding Mi-WT or Mi-E318K (clones 1 and 2). MW, molecular weight. **b**, **c**, Migration (**b**) and invasion (**c**) assays with 501mel melanoma cells described earlier. **d**, **e**, Migration and invasion (**e**) assays in RCC4 cells transduced with empty adenovirus (EV) or adenoviruses encoding either Mi-WT or Mi-E318K. **b**–**e**, Photographs above each bar graph show a representative field of the underside of filter after cell migration or invasion; magnification, ×200. **f**, **g**, Mi-E318K increased the number of colonies formed with Melan-a or RCC4 cells, respectively. Photographs of the colonies were taken at 2 weeks. **b**–**g**, Bars show the mean + s.d. of three replicate assays. **b**–**g**, Student's *t*-test compared Mi-WT to Mi-E318K. $*P < 0.05$, $**P < 0.01$ and $***P < 0.001$.

Mi-E318K was enhanced compared to wild-type-transfected or control cells. Overall, these data indicated that Mi-E318K was more potent than wild type for promoting invasive and tumorigenic behaviours in melanoma and RCC cells. However, Mi-E318K did not significantly stimulate melanoma or RCC cell growth (data not shown). These features are reminiscent of melanoma cell populations with increased invasive and division potential but with a slow growth rate, which are considered to be melanoma-initiating cells[22]. Thus, Mi-E318K might favour a phenotypic switch of melanoma cells towards a tumour-initiating cell phenotype, possibly in synergy with hypoxia[23].

Indeed, both the epidermis (where melanocytes are located) and the inner renal medulla are physiologically hypoxic tissues[24,25]. Hypoxia is capable of rapidly inducing HIF1A to initiate a cell-survival response[26]. Of note, several genes identified by expression profiling or ChIP-seq (*HIF1A*, *CCR7*, *HMOX1*) function in the hypoxia pathway. Both ultraviolet exposure and hypoxia generate radical oxygen species (ROS). In turn, oxidative stress activates inflammatory pathways that can lead to cellular transformation, proliferation and stem cell survival, among other features[27]. Our IPA analysis associated the Mi-E318K signature with inflammation, cell proliferation and cancer. Various environmental stresses, including hypoxia and ROS, were previously shown to induce global protein SUMOylation[28]. In this context, Mi-E318K, which prevents MITF SUMOylation, could impair the adaptation of cells to stress and initiate tumour formation. Our study has wide implications for understanding the role of MITF and its SUMOylation in the physiology and tumorigenesis of melanocytes and kidney cells.

We have identified a rare oncogenic germline substitution, Mi-E318K, that predisposes to both melanoma and RCC. Interestingly, *MITF* loss-of-function mutations are responsible for an inherited disorder in neural crest cell development, the type 2a Waardenburg syndrome[7]. This is reminiscent of the *RET* oncogene, in which activating germline mutations predispose to medullary thyroid carcinoma, but loss-of-function germline mutations predispose to Hirschsprung's disease, a congenital absence of enteric neurons in the gastrointestinal tract[29]. Our data indicate that mutation screening in genetically enriched patients is a powerful strategy to identify rare genetic variation that confers a moderate risk of cancer[30]. Lastly, it highlights the relevance of hereditary tumour models for shedding light on cell-growth-related signals and identifying cancer driver genes.

METHODS SUMMARY

Participants were included with the approval of an institutional review board. Sanger sequencing of *MITF* isoforms was performed in 62 melanoma + RCC cases. Mutations numbering referred to NCBI accession NM_000248.3. Wild-type or Mi-E318K genotyping was performed in 1,659 controls and 829 cases by TaqMan; positive samples were checked by Sanger sequencing. Genome-wide SNP data were genotyped by the Centre National de Génotypage (CNG, CEA) using Illumina technology. PCA was applied to the SNP data using EIGENSTRAT software. Immunohistochemistry was performed on melanoma and kidney fixed samples with anti-MITF antibody (Abcam, clone D5). Mutations in the two SUMO1 fixation sites, p.K182R and p.E318K, were generated with the QuickChange method in wild-type *MITF-M* and *MITF-A* isoforms and verified by sequencing. Plasmids were transfected into HEK293, 501mel, Melan-a and RCC4 cells with FuGENE 6 reagent (Roche Applied Science). Western blotting and immunofluorescence were performed with antibodies to MITF (Abcam, clone C5), HA-tag, SUMO1 or ERK2 (Santa Cruz Biotechnology). Reporter assays were performed by transient transfection in triplicate with lipofectamine (Invitrogen), and pCMVβGal was included to control transfection efficiency. Gene expression microarray assays were performed with Agilent technology by the Institut de Cancérologie Gustave Roussy (IGR) genomics platform. ChIP-seq experiments were performed by the Institut de Génétique et de Biologie Moléculaire et Cellulaire (IGBMC) microarray and sequencing platforms. Colony forming assays were performed after 14 days of culture; cells were fixed, stained with 0.4% crystal violet, and photographed. Statistical analyses for comparison of allele frequencies between cases and controls were performed with Fisher's exact test. All computations were performed with Stata software, version 11. For functional assays, statistical significance was evaluated with the Student's *t*-test. Results were considered significant when the Student's *t*-test, $*P$ value ≤ 0.05, $**P \leq 0.01$, $***P \leq 0.001$.

Full Methods and any associated references are available in the online version of the paper at www.nature.com/nature.

Received 1 February; accepted 2 September 2011.
Published online 19 October 2011.

1. Tucker, M. A. Melanoma epidemiology. *Hematol. Oncol. Clin. North Am.* **23,** 383–395 (2009).
2. Rini, B. I., Campbell, S. C. & Escudier, B. Renal cell carcinoma. *Lancet* **373,** 1119–1132 (2009).
3. Maubec, E. *et al.* Characteristics of the coexistence of melanoma and renal cell carcinoma. *Cancer* **116,** 5716–5724 (2010).
4. Garraway, L. A. *et al.* Integrative genomic analyses identify MITF as a lineage survival oncogene amplified in malignant melanoma. *Nature* **436,** 117–122 (2005).
5. Cheli, Y., Ohanna, M., Ballotti, R. & Bertolotto, C. 15-year quest in search for MITF target genes. *Pigment Cell Melanoma Res.* **23,** 27–40 (2009).
6. Linehan, W. M., Srinivasan, R. & Schmidt, L. S. The genetic basis of kidney cancer: a metabolic disease. *Nature Rev. Urol.* **7,** 277–285 (2010).
7. Hershey, C. L. & Fisher, D. E. Genomic analysis of the microphthalmia locus and identification of the MITF-J/Mitf-J isoform. *Gene* **347,** 73–82 (2005).
8. Camparo, P. *et al.* Renal translocation carcinomas: clinicopathologic, immunohistochemical, and gene expression profiling analysis of 31 cases with a review of the literature. *Am. J. Surg. Pathol.* **32,** 656–670 (2008).
9. Granter, S. R., Weilbaecher, K. N., Quigley, C. & Fisher, D. E. Role for microphthalmia transcription factor in the diagnosis of metastatic malignant melanoma. *Appl. Immunohistochem. Mol. Morphol.* **10,** 47–51 (2002).
10. Murakami, H. & Arnheiter, H. Sumoylation modulates transcriptional activity of MITF in a promoter-specific manner. *Pigment Cell Res.* **18,** 265–277 (2005).
11. Mullenders, J. *et al.* Interleukin-1R-associated kinase 2 is a novel modulator of the transforming growth factor β signaling cascade. *Mol. Cancer Res.* **8,** 592–603 (2010).
12. Yu, J. *et al.* PTEN regulation by Akt–EGR1–ARF–PTEN axis. *EMBO J.* **28,** 21–33 (2009).

13. Wysocki, P. J. *et al.* Gene-modified tumor vaccine secreting a designer cytokine Hyper-Interleukin-6 is an effective therapy in mice bearing orthotopic renal cell cancer. *Cancer Gene Ther.* **17,** 465–475 (2010).
14. Li, Y., Qiu, X., Zhang, S., Zhang, Q. & Wang, E. Hypoxia induced CCR7 expression via HIF-1α and HIF-2α correlates with migration and invasion in lung cancer cells. *Cancer Biol. Ther.* **8,** 322–330 (2009).
15. Liu, F. Y. *et al.* NF-κB participates in chemokine receptor 7-mediated cell survival in metastatic squamous cell carcinoma of the head and neck. *Oncol. Rep.* **25,** 383–391 (2011).
16. Schatton, T. *et al.* Identification of cells initiating human melanomas. *Nature* **451,** 345–349 (2008).
17. Yang, Z., Song, L. & Huang, C. Gadd45 proteins as critical signal transducers linking NF-κB to MAPK cascades. *Curr. Cancer Drug Targets* **9,** 915–930 (2009).
18. Datta, D., Banerjee, P., Gasser, M., Waaga-Gasser, A. M. & Pal, S. CXCR3-B can mediate growth-inhibitory signals in human renal cancer cells by down-regulating the expression of heme oxygenase-1. *J. Biol. Chem.* **285,** 36842–36848 (2010).
19. Was, H. *et al.* Overexpression of heme oxygenase-1 in murine melanoma: increased proliferation and viability of tumor cells, decreased survival of mice. *Am. J. Pathol.* **169,** 2181–2198 (2006).
20. Wang, M. J. & Lin, S. A region within the 5′-untranslated region of hypoxia-inducible factor-1α mRNA mediates its turnover in lung adenocarcinoma cells. *J. Biol. Chem.* **284,** 36500–36510 (2009).
21. Garcia-Dominguez, M. & Reyes, J. C. SUMO association with repressor complexes, emerging routes for transcriptional control. *Biochim. Biophys. Acta* **1789,** 451–459 (2009).
22. Hoek, K. S. & Goding, C. R. Cancer stem cells versus phenotype-switching in melanoma. *Pigment Cell Melanoma Res.* **23,** 746–759 (2010).
23. Li, Z. & Rich, J. N. Hypoxia and hypoxia inducible factors in cancer stem cell maintenance. *Curr. Top. Microbiol. Immunol.* **345,** 21–30 (2010).
24. Zou, A. P. & Cowley, A. W. Jr. Reactive oxygen species and molecular regulation of renal oxygenation. *Acta Physiol. Scand.* **179,** 233–241 (2003).
25. Bedogni, B. & Powell, M. B. Skin hypoxia: a promoting environmental factor in melanomagenesis. *Cell Cycle* **5,** 1258–1261 (2006).
26. Bellot, G. *et al.* Hypoxia-induced autophagy is mediated through hypoxia-inducible factor induction of BNIP3 and BNIP3L via their BH3 domains. *Mol. Cell. Biol.* **29,** 2570–2581 (2009).
27. Reuter, S., Gupta, S. C., Chaturvedi, M. M. & Aggarwal, B. B. Oxidative stress, inflammation, and cancer: how are they linked? *Free Radic. Biol. Med.* **49,** 1603–1616 (2010).
28. Tempé, D., Piechaczyk, M. & Bossis, G. SUMO under stress. *Biochem. Soc. Trans.* **36,** 874–878 (2008).
29. Manié, S., Santoro, M., Fusco, A. & Billaud, M. The RET receptor: function in development and dysfunction in congenital malformation. *Trends Genet.* **17,** 580–589 (2001).
30. Manolio, T. A. *et al.* Finding the missing heritability of complex diseases. *Nature* **461,** 747–753 (2009).

Supplementary Information is linked to the online version of the paper at www.nature.com/nature.

Acknowledgements We thank the patients and family members who participated in this study and the clinicians who identified these families, the French Familial Melanoma Study Group and the Inherited Predisposition to Kidney Cancer network. We acknowledge the contribution of the IGR Biobank for providing MELARISK samples and the CEPH Biobank for processing DNA samples. We thank L. Larue, J, Feunteun, A. Sarasin and E. Solary for critical reviews of the manuscript. We thank V. Lazar and S. Forget for coordination of the IGR's genomics and genetic platforms, N. Pata-Merci, V. Marty, S. Le Gras and A. Chabrier for their technical expertise, and M. Barrois for technical counselling. We also thank A. Boland for DNA extraction and quality control for genome-wide genotyping. This work was supported by grants from INSERM, Ligue Nationale Contre Le Cancer (PRE05/FD and PRE 09/FD) to F.D.; Programme Hospitalier de Recherche Clinique (PHRC 2007/AOM-07-195) to M.-F.A. and F.D.; ARC N°A09/5/5003 to B.B.-d.P.; ARC 4985 to C.B.; Institut National du Cancer (INCa)-Cancéropole Ile de France (melanoma network RS#13) to B.B.-deP.; INCa- PNES rein to B.G., S.Ga. and S.R., INCa grant R08009AP to C.B.; Fondation de France 2010 to R.B.; INCa and Ligue National Contre le Cancer to I.D., Fond de maturation IGR and Fondation Gustave Roussy to B.B.-d.P.; Société Française de Dermatologie SDF2004 to R.B. and P.B., SFD2009 to B.B.-d.P.; 2009 SGR 1337 from AGAUR, Generalitat de Catalunya, and FIS PS09/01393 from the Fondo de Investigaciones Sanitarias, Instituto de Salud Carlos III, Spain to S.P. and C.B.; and personal donations from C. and N. de Paillerets and M.-H.Wagner. to B.B.-d.P. B.B-d.P. holds an INSERM Research Fellowship for hospital-based scientists. Work at the Centre National de Génotypage (CNG) and Centre d'Etude du Polymorphisme Humain (CEPH) was supported in part by INCa.

Author Contributions C.B., F.L., M.L., F.D., R.B. and B.B.-d.P. designed the experiments and wrote the manuscript. A.Re., B.G., S.S. and G.M.L. participated in the scientific discussions. E.M., P.Va., S.D., N.P., T.M.-D., L.T., P.A.-B., N.D., F.B., A.Ro., J.-L.P., B.L., C.R., B.E., O.C., L.B., S.R., J.C., B.T., P.Gh., L.P., S.P., C.B., H.O., C.I., E.R., R.L. and P.B. collected biological samples. P.Ga. collected the control samples. F.L., M.d.L. and B.d'H. performed sequencing and genotyping of patients. H.B. supervised DNA extraction and quality control for genome-wide genotyping. D.Z. and M.L. were responsible for the genome-wide genotyping of cases and controls and genotyping of MITF variant in controls. E.C. carried out the analysis of SNP genotype data. F.D. supervised the statistical analysis of all genotyped data. K.B. and S.Gi. performed the functional analysis. A.d.l.F., V.M. and P.Vi. performed MITF immunostaining. T.S. and I.D. designed and performed the ChIP-seq experiments. P.D. performed the gene expression profiling analysis. M.-F.A. initiated the collection of melanoma and RCC cases. S.R. initiated the collection of RCC families. M.-F.A and F.D. initiated the MELARISK collection. H.M. and V.C. contributed to the management of the MELARISK database.

Author Information Genome data has been deposited at the European Genome-Phenome Archive (EGA; http://www.ebi.ac.uk/ega), which is hosted at the EBI, under accession number EGAS00000000048. Gene expression data related to this paper have been submitted to the Array Express repository at the European Bioinformatics Institute (http://www.ebi.ac.uk/arrayexpress/) under the accession number E-TABM-1198. Reprints and permissions information is available at www.nature.com/reprints. The authors declare no competing financial interests. Readers are welcome to comment on the online version of this article at www.nature.com/nature. Correspondence and requests for materials should be addressed to B.B.-d.P. (brigitte.bressac@igr.fr).

The French Familial Melanoma Study Group

François Aubin[1], Bertrand Bachollet[2], Céline Becuwe[3], Pascaline Berthet[4], Yves Jean Bignon[5], Valérie Bonadona[6], Jean-Louis Bonafe[7], Marie-Noëlle Bonnet-Dupeyron[8], Fréderic Cambazard[9], Jacqueline Chevrant-Breton[10], Isabelle Coupier[11], Sophie Dalac[12], Liliane Demange[13], Michel d'Incan[14], Catherine Dugast[15], Laurence Faivre[16], Lynda Vincent-Fétita[17], Marion Gauthier-Villars[18], Brigitte Gilbert[19], Florent Grange[20], Jean-Jacques Grob[21], Philippe Humbert[1], Nicolas Janin[22], Pascal Joly[23], Delphine Kerob[24], Christine Lasset[6], Dominique Leroux[25], Julien Levang[1], Jean-Marc Limacher[26], Cristina Livideanu[27], Michel Longy[28], Alain Lortholary[29], Dominique Stoppa-Lyonnet[18], Sandrine Mansard[14], Ludovic Mansuy[30], Karine Marrou[3], Christine Matéus[2], Christine Maugard[31], Nicolas Meyer[32], Catherine Nogues[33], Pierre Souteyrand[14], Laurence Venat-Bouvet[34] & Hélène Zattara[35]

[1]Centre Hospitalier Universitaire St Jacques, Dermatologie et Vénéréologie, 2 Place St Jacques, 25030 Besançon, France. [2]Institut de Cancérologie Gustave Roussy, Service de Dermatologie, 114 Rue Edouard Vaillant, 94805 Villejuif, France. [3]Hôpital de l'Hôtel-Dieu, Service de Dermatologie, 1 place de l'Hôpital, 69288 Lyon Cedex 2, France. [4]Service d'Oncologie Génétique, Centre François Baclesse, 3 Avenue du Général Harris, 14076 Caen Cedex 5, France. [5]Centre Hospitalier Jean Perrin, 58 rue Montalembert, BP 392, 63011 Clermont-Ferrand Cedex 1, France. [6]Centre Léon Bérard, Unité Clinique d'Oncologie Génétique, 28 Rue Laënnec, 69373 Lyon Cedex 8, France. [7]Unité de Dermatologie, Centre Hospitalier Universitaire de Rangueil, 1 avenue Jean Poulhès, TSA 50032, 31059 Toulouse, France. [8]Centre Hospitalier, Service de Génétique, 179 Boulevard Maréchal Juin, 26953 Valence Cedex 9, France [9]Centre Hospitalier Universitaire de St Etienne, Hôpital Nord, Service de Dermatologie, Vénéréologie, 42055 St Etienne Cedex 2, France. [10]Chru Pontchaillou, Service de Dermatologie, 35 Rue André Le Guillloux, 35033 Rennes, France. [11]Centre Hospitalier Universitaire Hôpital Arnaud de Villeneuve, Unité d'Oncogénétique, 371 Avenue Doyen Gaston Giraud, 34295 Montpellier Cedex 5, France. [12]Centre Hospitalier Universitaire Hôpital du Bocage, Service de Dermatologie, 2 boulevard Maréchal de Lattre de Tassigny, BP 77908, 21079 Dijon, France. [13]Polyclinique Courlancy, Service de Radiothérapie et Oncologie Médicale, 38 rue de Courlancy, 51000 Reims, France. [14]Centre Hospitalier Universitaire Estaing, Service de Dermatologie, 1 Place Lucie Aubrac, 63003 Clermont Ferrand Cedex 1, France. [15]Centre Eugene Marquis, Oncologie Génétique, Rue de la Bataille de Flandres Dunkerque, CS 44229, 35042 Rennes, France. [16]Centre Hospitalier Universitaire Hôpital du Bocage, Centre de Génétique, 2 Boulevard Maréchal de Lattre de Tassigny, BP77908, 21079 Dijon, France. [17]Hopital Cochin, Service de Dermatologie, Pavillon Tarnier, 89 rue d'Assas, 75006 Paris, France. [18]Institut Curie, Génétique Oncologique, 26 rue d'Ulm, 75248 Paris Cedex 5, France. [19]Centre Hospitalier Universitaire La Milétrie, Service de Génétique Médicale, 2 rue de la Milétrie, BP 577, 86021 Poitiers, France. [20]Hôpital Robert Debré, Service de Dermatologie U42, Avenue du Général Koenig, 51092 Reims, France. [21]Hôpital Sainte-Marguerite, Service de Dermatologie, 270 Boulevard Sainte-Marguerite, 13274 Marseille Cedex 9, France. [22]Centre Hospitalier Universitaire Sart Tilman, Département de Génétique Humaine, Centre Hospitalier Universitaire de Liege, 4000 Liege, Belgium. [23]Centre Hospitalier Universitaire de Rouen, Hôpitaux de Rouen, Clinique Dermatologique, Hôpital Charles Nicolle, 1 rue de Germont, 76031 Rouen, France. [24]Hopital Saint-Louis, Service de Dermatologie, 1 Avenue Claude Vellefaux, 75475 Paris Cedex 10, France. [25]Centre Hospitalier Universitaire de Grenoble, Hôpital Couple Enfant, Département de Génétique et Procréation, Génétique Clinique, Consultations d'Oncogénétique, BP 217-F, 38043 Grenoble Cedex 9, France. [26]Hôpital Pasteur, Hôpitaux civils de Colmar, Service d'Oncologie, 39 Avenue Liberté, 68024 Colmar, France. [27]Centre Hospitalier Universitaire Toulouse, Hopital Purpan, Service de Dermatologie, Place du Docteur Baylac TSA 40031, 31059 Toulouse Cedex 9, France. [28]Institut Bergonié, Laboratoire de Génétique Moléculaire, 229 cours de l'Argonne, 33076 Bordeaux, France. [29]Centre Catherine de Sienne, Oncologie Médicale, 2 rue Eric Tabarly, BP 20215, 44202 Nantes Cedex 2, France. [30]Centre Alexis Vautrin, Consultation Oncogénétique, UF Nancy 9901, 6 avenue de Bourgogne, 54511 Vandoeuvre Les Nancy, France. [31]Centre Hospitalier Universitaire de Strasbourg, Consultations d'Oncogénétique, Service d'Hématologie et d'Oncologie, 1 place de l'Hôpital, 67091 Strasbourg, France. [32]Centre Hospitalier Universitaire de Toulouse, Hôpital Larrey, Service de Dermatologie, Vénéréologie, 24 Chemin de Pouvourville, TSA 30030, 31059 Toulouse Cedex 9, France. [33]Centre René Huguenin, Service d'Oncogénétique, 35 rue Dailly, 92210 St Cloud, France. [34]Oncogénétique, Centre Hospitalier Universitaire de Limoges, Hôpital Universitaire de Dupuytren, 2 Avenue Martin Luther King, 87042 Limoges, France. [35]Département de Génétique Médicale, Hôpital de la Timone, Unité de Génétique Clinique, 264, rue St Pierre, 13005 Marseille, France.

METHODS

Study participants. Patients with melanoma and RCC. Sixty-two patients that had developed both melanoma and RCC were included in the MELARISK collection at the Institut de Cancérologie Gustave Roussy (IGR) and other French hospitals, 71% were males. None of these patients carried a germline *CDKN2A*, *CDK4* or *VHL* pathogenic mutation.

Patients with melanoma only. The patients with melanoma were enrolled through a nationwide network of French dermatology and oncogenetic clinics that constituted the Familial Melanoma Project and the MELARISK collection. The present study investigated a total of 371 index cases from independent pedigrees with a family history of melanoma (at least two melanoma cases) and/or pancreatic cancer, and 232 sporadic cases diagnosed with multiple primary malignant melanomas. A subset of the families ($N = 34$) included a melanoma patient and relatives with pancreatic cancer. These were part of the *CDKN2A* mutation testing procedure; carriers of the *CDKN2A* mutation have high risk of developing pancreatic cancer[31]. All cases had confirmed diagnoses of malignant melanoma through medical records, review of pathological material, and/or pathological reports. For all these patients, mutation screening for *CDKN2A* (exon 1β, 1α, 2 and 3) and *CDK4* (exon 2) had been undertaken for molecular diagnosis purposes. None of these patients carried a known *CDKN2A* or *CDK4* pathogenic mutation.

Patients with RCC only. Overall, 164 patients included in this study had developed RCC only. Those patients had been recruited through French urology and oncogenetic clinics, within the French National Cancer Institute's 'Inherited Predisposition to Kidney Cancer' network. They were considered 'genetically enriched' based on the following criteria: familial aggregation, young age of onset and rare histological subtypes. Out of the total of 164 patients, 79 had sporadic ccRCC, 54 had papillary renal cell carcinoma (PRCC; with 6 type I PRCC, 19 type II PRCC, 1 mixed type PRCC and 28 unknown histological subtypes of PRCC), 1 had a mixed RCC phenotypes (that is, papillary and ccRCC), 5 had juvenile RCC and 25 had RCC of unknown histological subtype. None of the 79 patients with ccRCC carried a *VHL* pathogenic germline mutation; none of the 19 patients with PRCCII carried a *FH* germline mutation; and none of the 6 patients with PRCCI carried a *MET* germline mutation.

Control subjects. Controls were supplemented by a population-based sample of 1,659 French subjects that had participated in the Supplementation in Vitamins and Mineral Antioxidants (SU.VI.MAX) study[32]. We confirmed that these subjects had not developed any cancer at the time of the present study.

The study was approved by an institutional review board (CCPPRB no. 01-09-05, Paris Necker) for the MELARISK collection and by the Ethical Committee of Le Kremlin-Bicêtre University Hospital, for the kidney cancer collection. It was conducted according to the Declaration of Helsinki Principles. All participating subjects signed informed consent and provided blood samples. After informed consent had been obtained from the subjects, DNA was extracted from peripheral blood lymphocytes with the QIAamp DNA Blood mini kit (QIAGEN), according to manufacturer guidelines.

***MITF* gene sequencing.** Sanger sequencing of *MITF* coding sequence, the intron–exon boundaries and the 8 alternative promoters was performed in DNA extracted from the blood of 62 patients affected with melanoma + RCC (primers available upon request) on a 3730 DNA Analyser (Applied Biosystems; ABI). Nucleotide number refers to the wild-type cDNA sequence of *MITF* (NM_000248.3) as reported in GenBank.

Genotyping of Mi-E318K. Genotyping was carried out with Taqman according to the manufacturer recommendations. Primers and probes were supplied in the Assay-by-Design by Applied Biosystems (ABI). PCR reactions were performed with 10 ng genomic DNA and 0.2 μmol l^{-1} TaqMan MGB probes. Probe 5′-VIC-ATCAAGCAA**G**AACCCG-3′ was designed to match the wild-type allele, and probe 5′-6-FAM-CAAGCAA**A**AACCCG-3′ was designed to match the mutant allele (underlined bold indicates the nucleotide at the mutation site). PCR thermocycling was performed on ABI thermocyclers, as follows: 95 °C for 15 min; 30 cycles of 95 °C for 15 s and 60 °C for 1 min. Assays were carried out in 96-well plates that included a negative control (with no DNA) and positive controls (DNA from subjects with Mi-E318K). Plates were read on a 7900HT Fast Real-Time PCR System (ABI) with Sequence Detection Software (ABI). Carriers of Mi-E318K were confirmed by Sanger sequencing with the above protocol and primers for *MITF* exon 9.

PCA of genome-wide SNP data. To verify that the association of Mi-E318K with melanoma and/or RCC was not influenced by population stratification, we carried out PCA of SNP data across the genome in cases and controls that had been genome-wide genotyped and satisfied stringent quality control criteria. A total of 1,628 controls and 569 cases affected with melanoma, RCC or both cancers were genotyped by the Centre National de Génotypage (CNG) using Illumina HumanHap300 Beadchip version 2 duo array for controls and Illumina Humancnv370k and Human660W-Quad arrays for cases. Samples were excluded for any of the following reasons: (1) a call rate of less than 97% of the total number of SNPs on the chip (222 samples); (2) sex as ascertained by genotyping not matching reported sex (10 samples); (3) heterozygosity on autosomes departing from the estimated expected value (7 samples); (4) relatedness with another sample (4 samples). This resulted in exclusion of 243 samples. PCA was then applied to 1,954 subjects that passed quality control using EIGENSTRAT software[33]. To identify individuals of non-European ethnicity, SNPs were thinned to reduce linkage disequilibrium and combined with the HapMap data of wide-ranging ethnicity. The first two principal components (PCs) clearly separated the HapMap data into distinct clusters according to ethnicity and identified 29 study samples of non-European ancestry who were excluded. The remaining 1,925 European ethnicity samples (1,389 controls, 536 cases) were analysed similarly without the Hapmap data. Plotting the first two principal components showed appropriate clustering of cases and controls (Supplementary Fig. 1).

MITF immunohistochemistry. Briefly, 4-μm tissue sections were cut from paraffin-embedded blocks, deparaffinized and rehydrated. RCC (patient ID numbers 10276, 24976, 11473, 21309, 21939, 25220, 26534; all in Supplementary Table 2) immunohistochemistry was performed with a three-step, avidin–biotin–peroxidase method. Staining was performed in an automated Dako Autostainer. Heat-mediated antigen retrieval was performed in 0.1 mol l^{-1} pH 6.0 citrate, and samples were heated in a water bath for 30 min in a Dakolink processor (Dako). Monoclonal mouse anti-human MITF (Clone D5, Dako, 1/100) was incubated with the samples for 30 min at room temperature (22 °C). SSM immunohistochemistry (patient ID numbers 19525, 24976, 10254, 15168, 15012, 21000, 22112, 27708 all in Supplementary Table 2 except number 27708 in Supplementary Fig. 1) was performed with a three-step avidin–biotin–alkaline-phosphatase method. Staining was performed in a Roche Diagnostics Benchmark XT automated stainer. Heat-mediated antigen retrieval was performed in the automat in cell conditioning solution 1 (Roche Diagnostics) for 1 h (Dako). Monoclonal mouse anti-Human MITF (Clone D5, Roche Diagnostics, pre-diluted) was incubated with samples for 16 min at room temperature. All slides were then counterstained with haematoxylin. Appropriate negative and positive controls were prepared in parallel.

Functional assays. Plasmids. The pcDNA3-Mi construct, which carried the M-MITF isoform and the 3M vector have been described previously[34]. The A-MITF isoform was a gift from H. Arnheiter (NIH). The *MITF* mutations, p.K182R and/or Mi-E318K, were generated with the QuickChange method (Stratagene) with the following sense primers and their reverse complements: Mi-K182R 5′-CTTCCCAACATAAGAAGGGAGCTCACAGC-3′; MI-E318K 5′-GGATCATCAAGCAAAAACCAGTTCTTGAG-3′. Mutations were confirmed by DNA sequencing. His–SUMO1 and HA–SUMO2 were a gift from A. Dejean and have been described elsewhere[35].

Cell cultures, transfections, and immunoblots. Human 501mel and A375 melanoma cells, human RCC4 cells and HEK293 cells were grown in DMEM supplemented with 7% FBS. Melan-a cells were cultured in RPMI 1640, 7% FCS, 200 nM TPA and 200 pM cholera toxin. All the cells were maintained at 37 °C in a humidified atmosphere containing 5% CO_2. HEK293 cells were cultured in 6-well dishes (10^4 cells per well) and transfected with the above-mentioned plasmids (2 μg of total DNA per well) and FuGENE 6 (Roche Applied Science). Forty-eight hours later, the cells were washed with PBS and lysed at 95 °C in 1× loading buffer (41.6 mM Tris, pH 6.8, 1.5% SDS, 6.7% glycerol). Proteins were resolved by electrophoresis in 10% SDS–polyacrylamide gels and transferred to PVDF membranes. Proteins were detected with ECL (Amersham) and antibodies to MITF (Abcam), HA-tag (Abcam), SUMO1 (Santa Cruz Biotechnology) or ERK2 (Santa Cruz Biotechnology).

Reporter assays. Human 501mel melanoma cells and HEK293 cells were seeded in 24-well dishes (25×10^3 cells per well). Subsequently, cells were transiently transfected with 0.3 μg reporter plasmid (3M, pHIF1A, pMET), 0.05 μg of MITF-encoding plasmids or empty, control pcDNA3 (EV), 2 μl of lipofectamine reagent (Invitrogen) and 0.05 μg of pCMVβGal for controlling the variability in transfection efficiency. Cells were lysed 48 h later and assayed for luciferase and β-galactosidase activities. Transfections were repeated at least three times.

Immunofluorescence. HEK293 cells were seeded on glass coverslips (100×10^3 cells) in 6-well dishes, and transfected with 3 μg of the different MITF mutants and 10 μl lipofectamine. Forty-eight hours later, cells were fixed for 10 min with 4% paraformaldehyde, permeabilized for 2 min with 0.1% Triton X-100/1% bovine serum albumin (BSA), and treated for 2 min with NH_4Cl 50 mM . Then, samples were washed three times in PBS and stained for 1 h with monoclonal anti-MITF antibody (Abcam, clone D5) in 1% BSA/PBS. Next, samples were washed three times in PBS for 5 min each and then stained secondarily for 1 h with Alexa-594-conjugated goat-anti-mouse antibody (Molecular probes) in 1% BSA. Cells were counterstained with 4,6-diamidino-2-phenylindole (DAPI), mounted with Fluoromount-G (Southern Biotech), and examined with a Zeiss Axiophot microscope equipped with epifluorescent illumination.

Colony forming assay. Immortalized Melan-a mouse melanocytes, A375 human melanoma cells and RCC4 human cells (8×10^4 cells per well) were transfected with wild type or Mi-E318K (3 μg total DNA per well and 10% pBABE-puro) with the FuGENE 6 Transfection reagent (Roche Applied Science). Puromycin (1 μg ml^{-1}) was added to media at 48 h post-transfection. Fourteen days later, the cells were fixed and stained with 0.4% crystal violet, and the plates were photographed.

Establishing stable 501mel cells that expressed tagged MITF. 501mel cells were transfected with FuGENE 6 reagent, a vector encoding puromycin resistance, and a pCMV vector that was either an empty, control vector or a vector encoding 3×HA-tagged MITF (wild type or Mi-E318K). Transfected cells were selected with puromycin; the expression of MITF was verified by western blot analysis with anti-MITF (Abcam, C5) or anti-HA (Roche, 12CA5) antibodies.

Migration and invasion assays. Migration (on uncoated filters) and invasion (on coated filters with matrigel) were investigated in a Boyden chamber system that comprised 24-well plates and 8-μm pore filter inserts (BD Bioscience). Stable 501mel melanoma cells (2×10^5 cells), A375 melanoma cells (1.5×10^5 cells) and RCC4 renal cancer cells (5×10^4 cells) were infected with control vector or adenovirus that encoded wild type or Mi-E318K at a multiplicity of infection (MOI) of 20 for 24 h, were then resuspended in serum-free DMEM and seeded on the upper chamber inserts. DMEM with 7% FCS was placed into the lower chamber. Twenty-four hours (501mel and RCC4) or 6 h (A375 cells) later, cells adherent to the underside of the filters were fixed with 4% PFA and stained with 0.4% crystal violet. Adherent cells were counted in five random fields at ×200 magnification. Results represented the average of duplicate samples from three independent experiments.

Gene expression arrays. Three replicates were performed for both RCC4 and A375 cells. mRNA was isolated with Trizol (Invitrogen) from A375 melanoma cells and from RCC4 cells infected with either control, wild type or Mi-E318K, according to standard procedures. Briefly, probes were synthesized from 500 ng of total RNA in two steps, according to the manufacturer's instructions. The two samples to be compared were labelled separately with different fluorescent dyes, cyanine-3 (Cy3) and cyanine-5 (Cy5). For each sample, 1 μg of purified cRNA labelled in cy5 was mixed with the same amount of cRNA labelled in cy3. Label incorporation was checked on a NanoDrop spectrophotometer. Hybridizations were performed with a dye-swap strategy on whole-human-genome dual colour 8 × 60K oligonucleotide microarrays (design 028004; Agilent Technologies). Feature extraction software provided by Agilent (version 10.7.3.1) was used to quantify the intensity of fluorescent images and to apply a linear/lowess normalization to correct for artefacts caused by nonlinear rates of dye incorporation and inconsistent relative fluorescence intensities between some green and red dyes. All data were imported into Resolver software (Rosetta Biosoftware) for database management, quality control, computational re-
combination of dye-swaps and statistical analysis. Mi-E318K specific signature was generated using the following parameters: intensity >50; fold change >1.5; P value <0.05. Functional analysis was carried out with the Ingenuity Pathway Analysis (Ingenuity System, http://www.ingenuity.com).

ChIP-seq. ChIP-seq was performed as previously described[36]. Briefly, chromatin was prepared from native 501mel cells or cells that stably expressed HA-tagged wild type or Mi-E318K. The isolated chromatin was HA-immunoprecipitated and sequenced with an Illumina GAIIx sequencer. The raw data were analysed with the Illumina Eland pipeline V1.6 programme. Peak detection was performed with MACS software (http://liulab.dfci.harvard.edu/MACS/), and the peaks were annotated with GPAT software (http://bips.u-strasbg.fr/GPAT/Gpat_home.html). Peak annotations were performed with a window that included ±20 kb from the coordinates at the beginning and end of RefSeq transcripts. The total number of reads for the wild-type data set was 1.7 fold higher than for the Mi-E318K data set. To facilitate quantitative comparisons, an appropriate number of reads was randomly removed from the wild-type data set to match the number present in the Mi-E318K data set. Subsequently, a quantitative comparison of the ChIP-seq data sets was performed with seqMINER[37]. Clustering was performed by counting the number of tags in a 36-bp sliding window for each ChIP-seq data set based on the coordinates of wild-type or Mi-E318K binding sites or on a reference sequence (RefSeq TSS). Only peaks with ≥10 reads were used for comparison. A matrix of binding sites and densities was generated and subjected to K-means clustering with the seqMINER programme.

Statistical analysis. Fisher's exact test was used to compare Mi-E318K allele frequencies between cases and controls and among different groups of cases. The odds ratios and confidence intervals associated with Mi-E318K carrier status were estimated by exact logistic regression. Logistic regression was also used to test for the effect of Mi-E318K on melanoma and/or RCC with and without adjusting for the first ten principal components estimated from genome-wide SNP data in patients and controls who were genome-wide genotyped and passed quality control. All computations were performed with Stata software, version 11 (StataCorp LP). For functional assays, results were considered significant when the Student's t-test, *P value was ≤0.05, **$P \leq 0.01$, ***$P \leq 0.001$.

31. Goldstein, A. M. *et al.* High-risk melanoma susceptibility genes and pancreatic cancer, neural system tumors, and uveal melanoma across GenoMEL. *Cancer Res.* **66,** 9818–9828 (2006).
32. Hercberg, S. *et al.* The SU.VI.MAX Study: a randomized, placebo-controlled trial of the health effects of antioxidant vitamins and minerals. *Arch. Intern. Med.* **164,** 2335–2342 (2004).
33. Patterson, N., Price, A. L. & Reich, D. Population structure and eigenanalysis. *PLoS Genet.* **2,** e190 (2006).
34. Bertolotto, C., Bille, K., Ortonne, J. P. & Ballotti, R. Regulation of tyrosinase gene expression by cAMP in B16 melanoma cells involves two CATGTG motifs surrounding the TATA box: implication of the microphthalmia gene product. *J. Cell Biol.* **134,** 747–755 (1996).
35. Bischof, O. *et al.* The E3 SUMO ligase PIASy is a regulator of cellular senescence and apoptosis. *Mol. Cell* **22,** 783–794 (2006).
36. Martianov, I. *et al.* Cell-specific occupancy of an extended repertoire of CREM and CREB binding loci in male germ cells. *BMC Genomics* **11,** 530 (2010).
37. Ye, T. *et al.* seqMINER: an integrated ChIP-seq data interpretation platform. *Nucleic Acids Res.* **39,** e35 (2011).

CORRIGENDUM

doi:10.1038/nature16158

Corrigendum: A SUMOylation-defective MITF germline mutation predisposes to melanoma and renal carcinoma

Corine Bertolotto, Fabienne Lesueur, Sandy Giuliano, Thomas Strub, Mahaut de Lichy, Karine Bille, Philippe Dessen, Benoit d'Hayer, Hamida Mohamdi, Audrey Remenieras, Eve Maubec, Arnaud de la Fouchardière, Vincent Molinié, Pierre Vabres, Stéphane Dalle, Nicolas Poulalhon, Tanguy Martin-Denavit, Luc Thomas, Pascale Andry-Benzaquen, Nicolas Dupin, Françoise Boitier, Annick Rossi, Jean-Luc Perrot, Bruno Labeille, Caroline Robert, Bernard Escudier, Olivier Caron, Laurence Brugières, Simon Saule, Betty Gardie, Sophie Gad, Stéphane Richard, Jérôme Couturier, Bin Tean Teh, Paola Ghiorzo, Lorenza Pastorino, Susana Puig, Celia Badenas, Hakan Olsson, Christian Ingvar, Etienne Rouleau, Rosette Lidereau, Philippe Bahadoran, Philippe Vielh, Eve Corda, Hélène Blanché, Diana Zelenika, Pilar Galan, The French Familial Melanoma Study Group, Valérie Chaudru, Gilbert M. Lenoir, Mark Lathrop, Irwin Davidson, Marie-Françoise Avril, Florence Demenais, Robert Ballotti & Brigitte Bressac-de Paillerets

Nature **480,** 94–98 (2011); doi:10.1038/nature10539

In this Letter, one image was mistakenly duplicated during preparation of the artwork. In the original Fig. 3d, the left image illustrating migration of RCC4 cells transduced with empty adenovirus (EV) at 24 h is a duplicate of the middle image showing migration of RCC4 cells transduced with an adenovirus encoding Mi-WT. The corrected images and migration graph are shown in Fig. 1 of this Corrigendum. This correction does not alter any of the conclusions, and the authors apologize for any confusion this may have caused. *Nature* has not received a response from the following authors to approve this Corrigendum: V.M., T.M.-D., A.Ro., P.B., E.C. and V.C., and C. Becuwe., J.-L.B., J.C.-B., S.D., C.D., J.L., and K.M. from The French Familial Melanoma Study Group (L.D. is deceased).

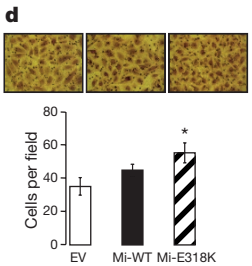

Figure 1 | This is the corrected Fig. 3d of the original Letter.